Int. J. High Technology Ceramics **4** (1988) 341–358

19

Ceramic Matrix Fibre Composites: Mechanical Testing and Performance

R. W. Davidge & J. J. R. Davies*

Building 552, Harwell Laboratory, Didcot, Oxfordshire OX11 0RA, UK

1 INTRODUCTION

Engineering ceramics are brittle. The failure strain is generally ~0·1% but exceptionally it can be as high as 0·5% in the strongest materials. Equivalent fracture stresses are in the range 250–2500 MPa (depending on Young's modulus). The elastic energy at fracture is proportional to the product of failure strain and fracture stress; thus the stronger the material, the more catastrophic the fracture process. Brittleness is associated with the low fracture energy of ceramics (typically a fracture toughness of 4 MPa $m^{1/2}$, or surface fracture energy or work of fracture of 40 J m^{-2}).

Several principles exist for increasing fracture toughness, for example through incorporation of particles of second phase, short whiskers, or transformation toughening particles of zirconia. Such effects are useful but modest, and increase toughness typically by a factor of 2–3. By far the most spectacular method of improving toughness is to reinforce a matrix with strong ceramic filaments. The fracture energy in the best materials can be increased by 3–4 orders of magnitude to give a work of fracture of 100 kJ m^{-2}. Such materials, however, are highly anisotropic, fail in a complex manner and often do not obey the basic concepts of fracture mechanics.

This paper discusses the state of knowledge on the mechanical properties and appropriate mechanical test methods for ceramic matrix composites (CMC) by reference to data on silicon-fibre-reinforced glass and glass ceramic matrices.

* To whom all correspondence should be addressed.

© 1988, UKAEA, Materials Development Division, Harwell.

2 UNIDIRECTIONAL COMPOSITES—BASIC BEHAVIOUR

2.1 Elastic behaviour

The Young's modulus E_c of a unidirectional (1-D) composite in direction 1 (Fig. 1), parallel to the fibres, is given to a good approximation by the law of mixtures assuming equal strains in the matrix and fibre:

$$E_c = E_f V_f + E_m V_m \tag{1}$$

where E_f, V_f, E_m, V_m are the Young's moduli and volume fractions of the fibre and matrix, respectively.

2.2 Tensile behaviour

Distinguishing features of successful CMC systems are that the failure strain of the fibres is significantly greater than that of the matrix and that the fibre is not too strongly bonded to the matrix. The matrix thus fractures at a stress σ_{mu} lower than the ultimate failure stress σ_{cu}. Typical stress–strain behaviour for material stressed in direction 1 in a tension parallel to the fibres is indicated in Fig. 2. For material with a reasonable density of inherent flaws and with zero fibre/matrix shear strength τ, the curve would follow the path

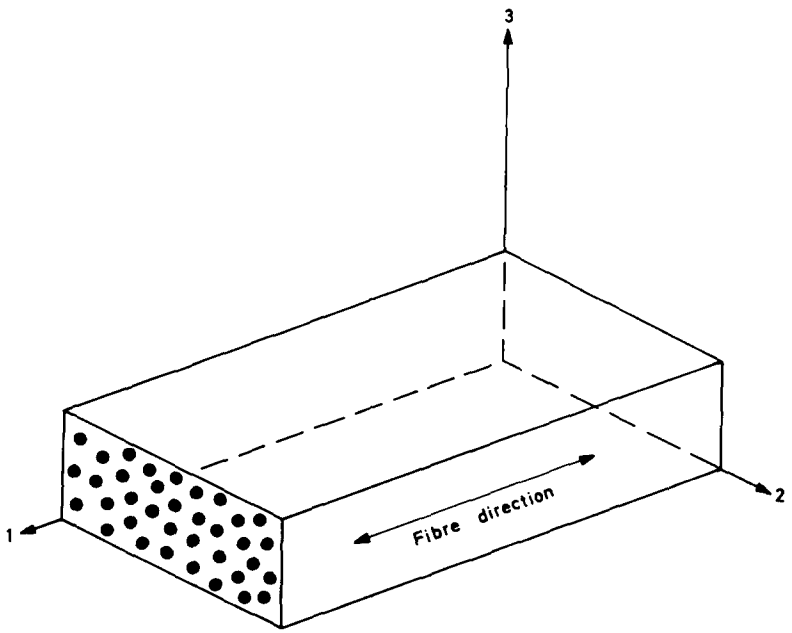

Fig. 1. Coordinate axes relating to unidirectional CMC.

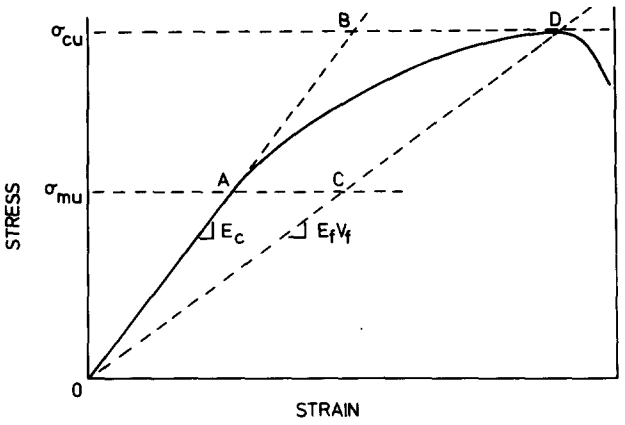

Fig. 2. Idealised stress–strain curve for tough CMC.

OACD. For other more realistic situations the curve from point A lies between the bounds AB and CD as indicated.

2.2.1 Matrix cracking

2.2.1.1 Energy balance approach (Aveston *et al.*, 1971; Hale & Kelly, 1972). Two conditions are necessary for a crack to form in the matrix. First, the work done by the applied stress must supply the energy required for the fracture process. Secondly, the stress in the matrix must reach the matrix fracture stress. Consider the situation in Fig. 3(a) where a single crack has been introduced completely through the matrix phase. Originally the strains in the fibre and matrix were equal but not the stresses (σ_f, σ_m):

$$\sigma_f = \sigma_m \frac{E_f}{E_m} \tag{2}$$

After introduction of the crack the stress originally on the matrix $V_m\sigma_m$ must be supported by the fibres. The stress on the fibre thus rises to

$$\sigma_f + \sigma_m \frac{V_m}{V_f} = \sigma_f\left(1 + \frac{E_m V_m}{E_f V_f}\right) = \sigma_f(1 + \alpha) \tag{3}$$

A number of energy changes then occur provided that slippage is possible at the fibre matrix interface. This is the usual situation; otherwise no fibre pull-out and toughening would occur. We thus have the situation in Fig. 3(b) where the stress on the fibres is enhanced over a distance $2x$ and that on the matrix is reduced.

We can now discuss the energy balance situation under constant load conditions. The composite expands as the matrix stresses relax and the work done ΔW is

$$\Delta W = E_f V_f \varepsilon_{mu}^2 x\, \alpha(1 + \alpha) \tag{4}$$

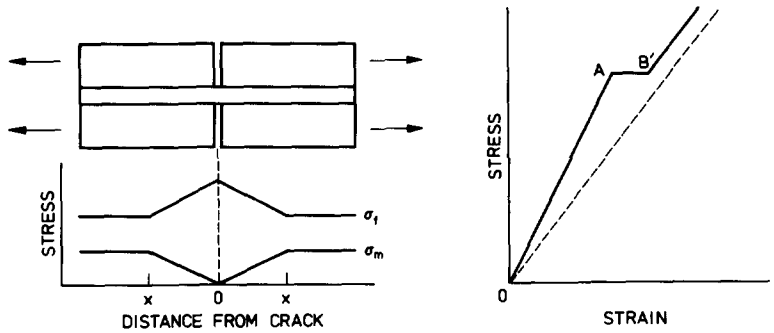

Fig. 3. (a) Single crack in CMC; and (b) localised effect on stress.

where ε_{mu} is the ultimate fracture strain of the matrix. The matrix loses elastic energy ΔE_m given by

$$\Delta E_m = \tfrac{2}{3} E_m V_m \varepsilon_{mu}^2 x \tag{5}$$

There is an increase in elastic energy in fibres ΔE_f

$$\Delta E_f = E_f V_f \varepsilon_{mu}^2 x\, \alpha(1 + \alpha/3) \tag{6}$$

The matrix slides back over the fibre absorbing energy ΔE_i at the interface as work is done against the fibre/matrix frictional force τ

$$\Delta E_i = \frac{2V_f}{3r} \tau \varepsilon_{mu} x^2 (1 + \alpha) \tag{7}$$

where r is the fibre radius. The crack can form only if

$$2\gamma_m V_m + \Delta E_i < \Delta W + \Delta E_m + \Delta E_f$$

and

$$< \tfrac{2}{3} E_c \varepsilon_{mu}^2 x \alpha \tag{8}$$

where γ_m is the surface energy of the matrix. The variable x is given by

$$x = \frac{E_f \varepsilon_{mu} \alpha r}{2\tau} \tag{9}$$

We thus find that the matrix failure strain for the composite will be enhanced when

$$\varepsilon_{mu}^3 < 12\tau\gamma_m \left(\frac{V_f^2}{rV_m}\right)\left(\frac{E_f}{E_c E_m^2}\right) \tag{10}$$

In this case the matrix will crack at the strain indicated by the right hand side of eqn (10). This is favoured by a high volume fraction of fibres of small radius. Further increase in strain then results in the matrix being traversed

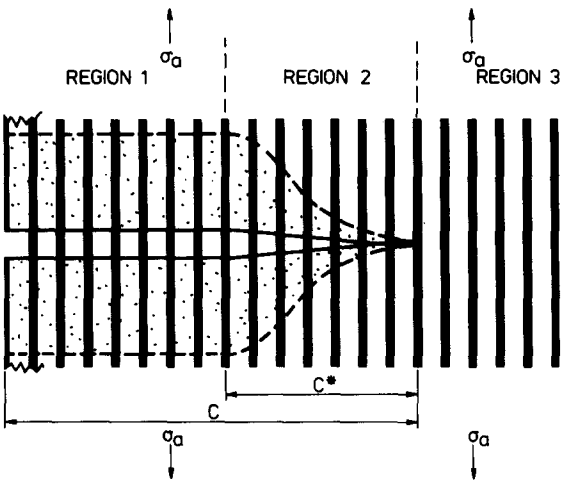

Fig. 4. Microcrack parallel to fibres under applied stress σ_a. Stippled area indicates zone where fibre matrix slippage has occurred.

by a series of cracks normal to the fibres, where the crack spacing lies between x and $2x$ given in eqn (9).

The above discussion simply demonstrates that matrix cracking is energetically favourable but for it to occur a microcrack of sufficient size must be present to raise the stress locally to the theoretical strength of the matrix. To examine how large the critical microcrack needs to be, a fracture mechanics approach requires discussion as presented below.

2.2.1.2 Fracture mechanics approach (*Marshall* et al., *1985*; *Budiansky* et al., *1986*; *Evans & McMeeking, 1986*; *McCartney, 1987*). The situation to be considered is shown in Fig. 4. The crack of length C has passed some way through the material. There are three distinct regions. Remote from the crack (Region 3) the material is unaffected by the presence of the crack. At the mouth of the crack (Region 1) the crack is fully established and the crack faces have relaxed to a constant crack opening displacement. Near the crack tip (Region 2) there is a transition between the two outer zones. Only recently have the fracture mechanics been solved, initially by Marshall *et al.* (1985) and more rigorously by McCartney (1987). The details of the analysis are too lengthy for consideration here but lead to the extremely important result that, for an established crack as in Fig. 4, the stress to propagate the crack is given by

$$\sigma_m = \frac{12\tau\gamma_m}{r}\left(\frac{V_f^2}{V_m}\frac{E_f(1-v^2)^2}{E_c E_m^2}\right)^{1/3}\frac{E_c}{1-v^2} \tag{11}$$

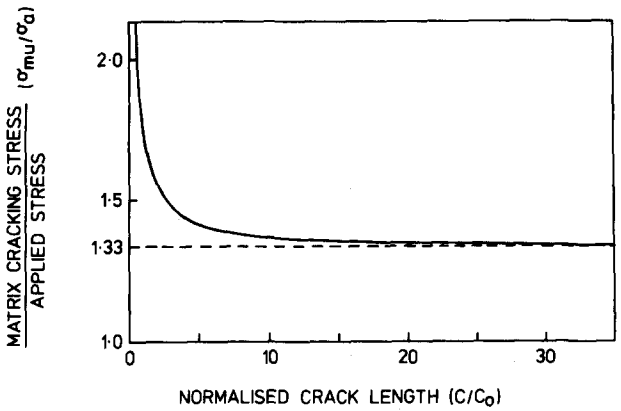

Fig. 5. Matrix cracking stress vs normalised crack length (Prewo & Brennan, 1982).

which is identical to that given in eqn (10) with an extra Poisson's ratio term for plane strain conditions.

The situation is to be contrasted strongly with that for unreinforced materials where the stress at the tip of the crack increases with increase in crack length. For these composite systems the stress at the tip of the crack is independent of crack length once the crack is longer than the necessary length $\dot{C}$ to reach the equilibrium situation. Thus matrix cracking is impossible below the threshold stress (eqn (11)) no matter how large the pre-existing defect. Obviously when $C < \dot{C}$ the stress enhancement at the crack tip is insufficient to reach the matrix cracking stress. Composites with intrinsic flaws less than this size will be expected to have a matrix cracking stress greater than that in eqn (11), as indicated in Fig. 5.

The significance of this analysis is that it is now possible to define the matrix cracking stress as an intrinsic property of the composite. Furthermore, the dimension of the matrix crack can be calculated for the transition point between crack-size-dependent behaviour and crack-size-independent behaviour.

The results of this theory have been compared with available experimental data for a number of systems (Marshall *et al.*, 1985; McCartney, 1987). There is good general agreement between the calculated matrix cracking stress and that observed experimentally. Interestingly the threshold crack size $\dot{C}$ is usually several times larger than the average fibre spacing which is the order of the expected inherent flaw size. The equivalence between the predicted and observed matrix cracking stresses suggests that inherent cracks of this size are in fact present.

2.2.2 Fibre failure and ultimate strength

At stresses greater than σ_{mu} and depending on the density and size of

inherent crack sources, the matrix will crack up into a series of parallel-sided blocks of width between x and $2x$. The ultimate strength of the composite σ_{mu} depends on the strength of the fibres σ_{fu}, such that

$$\sigma_{cu} = \sigma_{fu} V_f \tag{12}$$

Note that at σ_{cu} some of the load is still carried by the matrix in the unbroken regions and that the maximum stress on the fibres is restricted to the bridging regions between single matrix cracks. σ_{fu} may thus be greater than the value obtained for unrestrained fibres.

2.2.3 Work of fracture

When the stress σ_{cu} is reached, the fibres break and a controlled fracture results as the broken fibres are pulled out of the matrix. The two major processes contributing to the work of fracture (γ_f) of the composite are debonding and pull-out. The debonding term is generally insignificant compared to the pull-out term and can be neglected here (Hale & Kelly, 1972). A fibre embedded in the matrix will be pulled out if the embedded length is less than a critical length l_c, where τ is the fibre/matrix frictional stress:

$$l_c = \frac{\sigma_f r}{2\tau} \tag{13}$$

The work to pull out a single fibre W_f is

$$W_f = \pi l_c^2 r \tau \tag{14}$$

There are $V_f/\pi r^2$ fibres per unit area and assuming that the average pulled-out length is $l_c/2$

$$\gamma_f = \frac{V_f l_c^2 \tau}{3r} \tag{15}$$

or combining eqns (13) and (15) gives

$$\gamma_f = \frac{V_f \sigma_f^2 r}{12\tau} \tag{16}$$

Note that a high work of fracture is favoured by a large fibre radius and a low fibre/matrix shear strength: this is the reverse of the requirements for a high matrix cracking strain (eqn (10)).

3 TEST METHODS (Phillips & Davidge, 1986)

During the development of composite systems, relatively simple tests are usually appropriate. Consequently, most measurements of strength have

been carried out adequately by flexural testing. Two points have to be taken into consideration when carrying out such a test. First, unlike a simple ceramic, the compression strength of a ceramic matrix fibre composite may be similar to, or even less than the tensile strength. Secondly, the shear strength of planes parallel to fibres are generally very much less than the tensile or compressive strength parallel to fibres.

3.1 Bend tests

When a rectangular bar is loaded in 3-point bending the maximum tensile (σ_t) and compressive (σ_c) stresses occur at the surfaces under the middle loading point and are given to a first approximation by

$$\sigma_{11} = \sigma_t = \sigma_c = \frac{3Fl_k}{2bd^2} \tag{17}$$

where F is the fracture force, l_k the knife edge span and b and d the breadth and depth of the bar, respectively: the maximum shear stresses (τ) occur on the neutral plane and are

$$\sigma_{13} = \tau = \frac{3F}{4bd} \tag{18}$$

The ratio of tensile (or compressive) stress to shear stress ($\sigma_t : \tau$) is $2l_k/d$, and as the load is increased failure occurs when one of these reaches its critical value. Therefore the mode of failure depends on the relative value of tensile, compressive and shear strengths and the span : depth ratio ($l_k : d$) of the beam and, to an approximation, tensile (or compressive) failure will occur if $l_k/d > (\sigma_t)_{ult}/\tau_{ult}$ and shear failure if $l_k/d < (\sigma_t)_{ult}/\tau_{ult}$.

If approximate values of these strengths are known then an appropriate geometry can be defined. As a rough working rule, tension or compression failure will occur at $l_k/d > 20$ and shear failure at $l_k/d < 5$. It is however very important in this, as in all other fracture tests on fibre composites, to examine the specimen after failure to confirm that failure has occurred in the assumed mode and this point cannot be over-emphasised.

The flexural test is the most useful test during the development stage of a ceramic matrix/fibre composite system. It can be carried out with small, easily prepared specimens; it requires only standard testing machines and simple jigs; and it is readily adapted to high-temperature testing. The 4-point bend test is better for tensile/compressive properties because failure occurs away from the loading point. Matrix cracking can be identified from non-linearities in the load-displacement curve. The short span 3-point bend test gives a measure of the shear strength which compares well with other more complicated measurements.

3.2 Tensile strength

The main problems in measuring the tensile strength of a fibre composite are obtaining good alignment and ensuring that a valid tensile failure occurs without premature splitting parallel to the fibres. Splitting can occur either because of shear stresses arising from the specimen geometry or, if compressive wedge grips are used, by indentation of the grip surface serrations into the specimen. This latter problem is avoided by bonding end tabs on to the specimen to cushion the specimen and the most usual cause of premature splitting is the shear stresses arising from the loading system. Generally, the specimen is gripped at its ends by wedge grips and the load is imparted through shear stresses at the grip/specimen surface. The specimen is usually waisted to ensure failure in the gauge section away from the grip and splitting occurs if the shear stresses in the varying section reach the shear strength before the tensile stresses reach the tensile strength.

3.3 Transverse tensile strength

The transverse tensile strength (σ_{22}, σ_{33}), perpendicular to fibres, of 1-D CMC tends to be very low compared with the tensile strength in the fibre direction (σ_{11}), probably because the poor bonding between fibres and matrix and the brittleness of the matrix. The problems of measurement are similar to those of weak, homogeneous ceramics and the flexural test has much to offer because of its simplicity and adaptability to high-temperature testing. Further, unlike the measurement of σ_{11}, it will not suffer from the ambiguity of compression or in-plan shear failure.

3.4 Shear strength

Shear test methods can be divided into two groups, those using flat plate specimens and those using tubular or circular section specimens.

The simplest technique is the short beam interlaminar shear test described above in which a beam of low aspect ratio is subjected to 3-point bending. This technique yields values of strength which compare well with other tests and is most easily adapted to high-temperature testing. However it is not suitable for measuring shear modulus. Another disadvantage is that frequently it results in a mixed mode of failure.

A more satisfactory method for room-temperature testing is the torsion test (Burt, 1975). Ideally a thin-walled tube is twisted about its axis. If the ratio of tube radius to wall thickness is greater than 12 and one end of the

tube is free to move in the direction of the tube axis, a reasonably pure state of shear exists. Profiled end fittings are required to reduce the stress concentration factor and obtain valid failures. The shear strength can be obtained from the torque at failure and the shear modulus can be obtained either by strain-gauging the specimen or from the torque–twist curve. The tubes can be made up of unidirectional fibres either hoop-wound, or parallel to the axis. The test can also be carried out with solid rods (Hancox, 1972).

3.5 Compression strength

Unlike homogeneous, isotropic ceramics, measurement of the compressive strength of composites is one of the more difficult intrinsic material properties to measure and results tend to be very dependent on the loading geometry and testing conditions (Wolstencroft *et al.*, 1981). The main problems are buckling, 'brooming' of ends in solid column specimens, and axial alignment. In order to achieve accurate measurements of compression strength, complex loading fixtures and specimen configurations have been developed.

The effect of buckling manifests itself as a decrease in strength as the ratio of unsupported length to thickness increases. A reduction of this ratio results in higher strength but in practice a compromise may have to be sought between the need to eliminate buckling and the need to avoid end effects while leaving adequate space for strain gauges. Calculation of the critical length below which there is no contribution from buckling is not straightforward because the length depends on end constraint factors, which are not readily assessed.

Specimen brooming is usually overcome by using compressive wedge action grips and load introduction tabs bonded over a large area of the specimen. Axial alignment is important as any misalignment will introduce a bending load and cause the apparent strength to drop.

3.6 Toughness testing

In recent years it has become increasingly conventional to employ the vocabulary of linear elastic fracture mechanics in the technology of advanced ceramics, and to measure a critical stress intensity factor K_{IC} which is often referred to as 'fracture toughness'. The danger in applying this approach uncritically to CMC is that linear elastic fracture mechanics on the macroscopic scale is not generally applicable because: failure is a complex, unlocalised process, involving a multiplicity of cracks away from the major

macroscopic separation zone; and failure from a pre-existing crack does not, in general, occur by self-similar crack growth.

The idea of a toughness parameteter should not be discarded because it can still be useful in guiding material development, although at present it cannot be used with any precision as a parameter in design. It is more useful to realise that toughness can be measured in a number of ways which are all related in that they are each a measure of the amount of work which must be done in order to fracture the material.

Along these lines, as an aid to materials development, there is much to commend the work of fracture test (Tattersall & Tappin, 1966) for measuring the work done when fracture occurs on a plane perpendicular to fibres. In this test a notched beam is loaded in bending. The notch is preferably chevron-shaped or possibly straight and the specimen length, depth and notch size are defined so that, when the specimen is loaded in a hard testing machine, failure occurs in a controlled manner. The work of fracture, which approximates to the fracture surface energy, is then given by the work done during fracture divided by the area of fracture surface created. For notched beams of unidirectional composite tested in bending, cracks often deviate to run parallel to the fibres in a low energy configuration. This can be inhibited by using a circumferential notch.

For multi-angle laminates the situation is more complicated. Attempts to relate strength to the size of a major stress concentration, such as an artificial crack or a hole have not been generally successful. A wide range of linear elastic fracture mechanics type specimens had been used, such as edge-notch, centre-notch, compact tension, etc., but the data have been found, usually, to be dependent on geometry and not true materials parameters. Thus the data cannot be used in engineering design. However they can be useful in providing a semi-quantitative comparative assessment of the damage tolerance of composites, although in this case it is important to examine the specimens after fracture to determine the morphology of fracture, and to relate it to fabrication parameters.

3.7 Damage tolerance

This is clearly an important area of research in the future for ceramic matrix composites as many of their proposed applications may expose them to the possibility of impact damage. One way of approaching this is to introduce damage in a standardised way, for example by static indentation or drop-weight impact, and then to measure the strength of the material after impact. This is closely related to the concepts of toughness used for homogeneous ceramic materials: the more damage tolerant the material, the less its notch-sensitivity, and the greater its toughness.

4 EXPERIMENTAL DATA

4.1 Glass matrix

The filament-winding techniques developed originally for carbon fibres have been used extensively for the production of glass and glass ceramic matrix composites. The strongest material is borosilicate glass/SiC filament, where the expansion coefficients of the matrix and fibre are closely matched and the chemical interaction between the fibres and matrix can be controlled to give good interfacial shear behaviour. A typical stress–strain curve in bending for Nicalon-SiC-reinforced borosilicate glass is shown in Fig. 6 (Dawson *et al.*, 1987). Significant deviation from linear behaviour due to matrix cracking occurs at stresses ~ 800 MPa and the maximum nominal stress is ~ 1300 MPa. The value of V_f is 0·49 for this material and the maximum stress is very close to that expected from the strength of the fibres themselves according to eqn (12). This indicates that there is no great physical or chemical damage to the fibres during the processing operations. It should be noted that bend tests over-estimate the strength because of the lower elastic modulus near the tensile face due to matrix microcracking. The material has a very fibrous fracture mechanism which leads to a high work of fracture of 70 kJ m^{-2}. Figure 7 shows a micrograph of the tensile face at a strain of 2·5%. The matrix microcracks are clearly visible with a spacing $\sim 45\,\mu$m. In this view the matrix has powdered away from the fibres and the long pull-out fibre length is clearly visible.

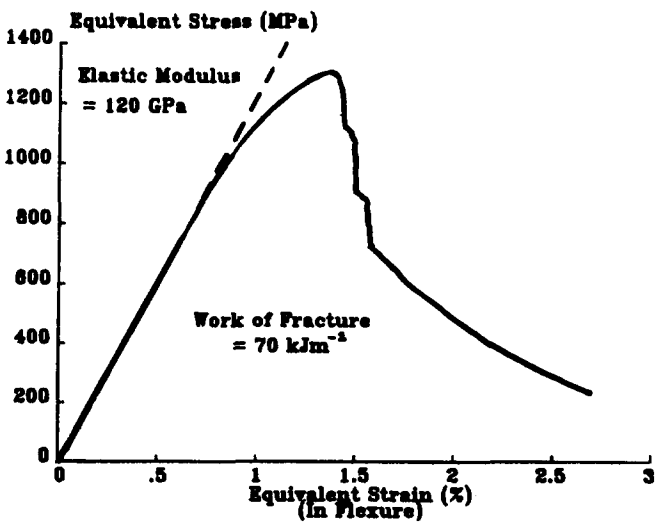

Fig. 6. Stress–strain curve in bending for borosilicate glass reinforced with 49% Nicalon silicon carbide fibres (Marshall, 1986).

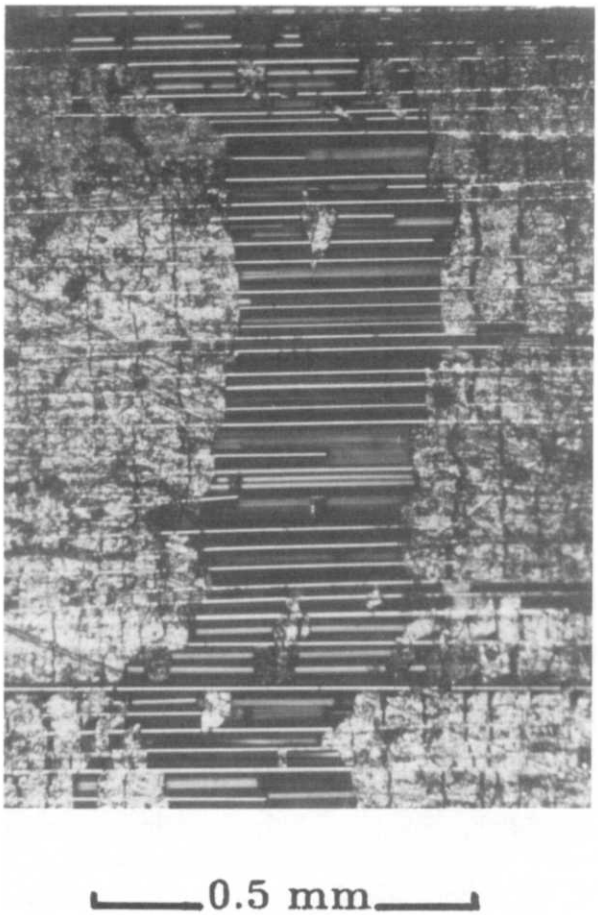

Fig. 7. Tensile face of material in Fig. 6 after strain of 2·5% (Marshall, 1986).

Figure 8 shows that this material has excellent reproducibility. Strength data for specimens prepared from 20 winding operations and 40 hot-pressed plates are plotted statistically. The standard deviation is 50 MPa and the Weibull modulus is 30. For specimens individually machined from an individual plate an even higher Weibull modulus of 40 has been obtained. Note also that the experimental points deviate from the line at low strength values which is indicative of a minimum strength or ultimate failure. This behaviour is vastly different from that of monolithic ceramics where the Weibull moduli are very much smaller. This is no doubt associated with the cooperative nature of the fracture in CMC which depends on the behaviour of a large number of separate fibres, in contrast to propagation from the single largest flaw in normal ceramics.

The fibre matrix interfacial shear strength can be calculated from

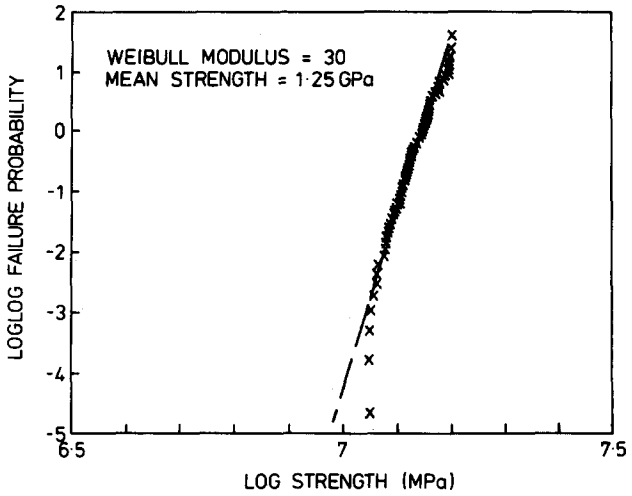

Fig. 8. Apparent maximum bend strength data for material in Fig. 6 plotted on Weibull probability axes (Marshall, 1986).

eqn (11) substituting $\gamma_m = 8\,J\,m^{-2}$ (Davidge & Tappin, 1968), $V_f = 0{\cdot}49$, $E_f = 200\,GPa$, $r = 6\,\mu m$, $V_m = 0{\cdot}51$, $E_m = 70\,GPa$, $E_c = 120\,GPa$ and $\varepsilon_{mu} = 0{\cdot}005$. This gives $\tau = 47\,MPa$.

A second way of measuring the interfacial shear stress is from the matrix cracking spacing from eqn (9). With $x = 30\,\mu m$ and $\sigma_f = 2{\cdot}5\,GPa$ this gives $\tau = 35\,MPa$. These two values are in very good agreement given the approximations of the calculations. Note that these shear strength values relate to a debonding of the fibre from the matrix with subsequent sliding. The above calculations measure the greater of these two quantities. On the other hand fibre pull-out relates to the frictional stress between the fibre and matrix when the fibre has generally debonded. The pull-out length is ~ 1 mm (Dawson *et al.*, 1987) and substitution into eqn (13) gives a lower value for τ of 8 MPa.

These interfacial properties of the material are easily controllable via the fabrication parameters, and the final composite properties may be thereby altered.

Materials with a borosilicate matrix have a limited temperature capability around 600°C, although the properties are well maintained to this temperature. Glass ceramic matrices are thus of obvious interest to increase the temperature capability of the material.

4.2 Glass ceramic matrices

Much of the development work (Brennan & Prewo, 1982; Prewo & Brennan, 1982; Prewo, 1986; Prewo *et al.*, 1986) has been on lithium aluminosilicate

matrices where the major crystalline phase is β-spodumene. The maximum useful temperature in composite form is $\sim$10–1200°C. Other matrices of interest include cordierite ($2\,MgO.2\,Al_2O_3 5SiO_2$), barium osumilite ($BaO\ 2MgO\ 3Al_2O_3\ nSiO_2$), mullite ($3Al_2O_3\ 2SiO_2$) and celsian ($BaO\ Al_2O_3\ 2SiO_2$). The latter materials could in principle be suitable to 15–1700°C. Filament-winding techniques are again used but the hot-pressing operation is done normally with the matrix in a glass form. A subsequent heat treatment or controlled cooling procedure is used to induce crystallisation so that in subsequent use the material has good refractory properties.

Bend or tensile testing of CMC obviously shows the materials in their best light where fracture is normal to reinforcing fibres. Unidirectional composites are unlikely to be used in many applications simply because the strength in a direction normal to the fibres is extremely low (20 MPa) as indicated (Marshall & Evans, 1985; Sbaizero & Evans, 1986) in Fig. 9. For most practical applications at least 2-D lay-ups will be used and some tensile results for 0°/90° and 45°/45° tensile tests are illustrated in Fig. 9 in contrast to tensile tests on 1-D composites. Some limited information is available for 3-D materials (Ko & Koczak, 1987).

The 2-D materials are the simplest lay-ups appropriate to shell type structures and it is important to understand the various features of the failure mechanisms. For the 0°/90° (Fig. 9) material there is a deviation from linearity at a stress $\sigma_d \approx 70$ MPa. This is followed by a succession of small load drops. These effects become more severe at a higher stress σ_m 130 MPa with a further decrease in specimen stiffness. The ultimate strength σ_f is

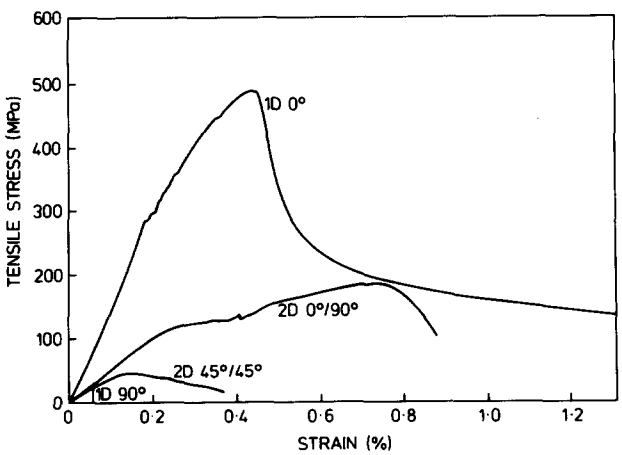

Fig. 9. Tensile stress–strain curves for lithium aluminosilicate glass ceramic reinforced with 50% Nicalon silicon carbide fibres in various 1-D and 2-D orientations.

180 MPa and progressive controlled failure occurs at higher strains. The sequence of failure modes is that delamination cracks between the various layers occurs around σ_d. Near the higher stress σ_m transverse cracks between the fibres appear in the 90° layers. Some of these then begin to propagate at higher strains across the 0° layers until the maximum stress is reached. In the latter stages the cracks propagating normal to the stress are impeded by the delamination cracks parallel to the stress. The failure at the maximum stress is identifed with the failure of the fibres in the 0° direction. Simplistically, one would expect the ultimate strength of the 2-D material to be 50% of the 1-D material, that is 250 MPa, rather than the 180 MPa observed. The reasons for this are not fully understood but residual stresses in such lay-ups may be one cause.

The 45°/45° material behaves in a relatively simple manner with linear behaviour up to near the maximum fracture stress at 40 MPa.

There is an interesting contrast in interfacial shear properties of this material when compared with the glass matrix material. The interfacial shear stress has been calculated by a number of techniques including individual indentations on ends of fibres (Marshall, 1986; Marshall & Oliver, 1987), and also values calculated from the matrix crack spacing and the matrix cracking stress as described above. These calculations gave a shear stress value of only 2 MPa. Note that modest variations in the matrix cracking strain give a very large difference in shear stress due to the cube root term in eqn (10). In these materials the debonding stress may be very low because of the fabrication methods. Crystallisation of the matrix usually involves a volume change which could lead to alterations in the nature of the

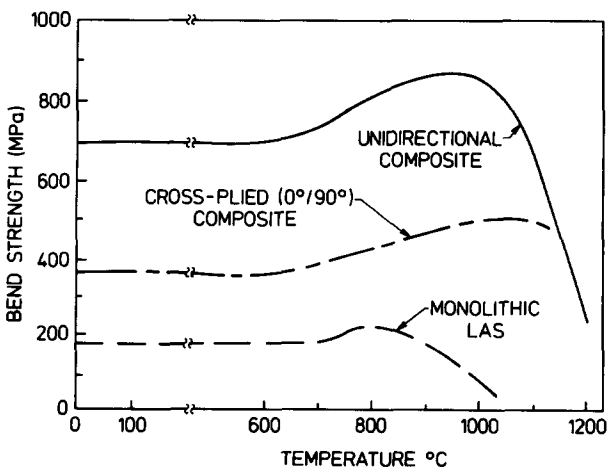

Fig. 10. Temperature-dependence of strength for lithium aluminosilicate glass ceramic reinforced with 50% Nicalon silicon carbide fibres.

interface. The value of 2 MPa may thus relate to sliding rather than debonding.

The temperature-dependence of the bend strength of such material is shown in Fig. 10 both for unidirectional material 0°/90° crossply material and the plain lithium aluminosilicate glass (Brennan & Prewo, 1982). Strengths are not as high as for the glass system but the properties are maintained in composite form to ~1000°C. At 1000°C there is a significant increase in the interfacial fibre/matrix shear strength due to oxidation and the material becomes notch-sensitive (Yuh & Evans, 1987).

5 CONCLUSION

The field of CMC is still at a relatively early stage of development but already several promising materials exist with potential for engineering applications. For 1-D material there is good agreement between theory and experimental data for simple mechanical tests. The situation is less well understood for 2-D and 3-D materials. Most testing carried out to date has been for process optimisation, and has been of the simplest possible type, i.e. flexural testing. The protracted nature of failure in these materials leads to difficulties in the application of popular concepts such as toughness. Therefore production of definitive engineering data requires a clear understanding of the events leading up to failure as well as the failure mode itself. Little information exists for a wide range of mechanical behaviour including creep, fatigue, and impact; criteria for prediction of engineering performance are essential in these areas. There is thus clearly a detailed need for further research and development on this class of material.

ACKNOWLEDGEMENT

Financial support from the Department of Trade and Industry under the Harwell Materials Engineering Project is gratefully acknowedged.

REFERENCES

Aveston, J., Cooper, G. A. & Kelly, A. (1971). *Proc. Conf. The Properties of Fibre Composites.* IPC Science & Technology Press, Guildford, UK, pp. 15–26.

Brennan, J. J. & Prewo, K. M. (1982). *J. Mat. Sci.*, **17**, 2371–83.

Budiansky, B., Hutchinson, J. W. & Evans, A. G. (1986). *J. Mech. Phys. Solids*, **34**, 167–89.

Burt, C. W. (1975). Experimental characterisation of composites in composite materials 8. *Structural Design & Analysis Part 2*, ed. C. C. Chamis, Academic Press, London.
Davidge, R. W. & Tappin, G. (1968). *J. Mat. Sci.*, **3**, 165–73.
Dawson, D. M., Preston, R. F. & Purser, A. (1987). *Ceram. Eng. Sci. Proc.*, **8**, 815–21.
Evans, A. G. & McMeeking, R. M. (1986). *Acta Met.*, **34**, 2435–41.
Ford, B., Cooke, R. G. & Newsam, S.(1987). *Brit. Ceram. Proc.*, **39** (in press).
Hale, D. K. & Kelly, A. (1972). *Ann. Rev. Mat. Sci.*, **2**, 405–62.
Hancox, N. L. (1972). *J. Mat. Sci.*, **7**, 1030–40.
Ko, F. & Koczak, M. (1987). *Ceram. Eng. Sci. Proc.*, **8**, 822–33.
Marshall, D. B. (1986). *J. Amer. Ceram. Soc.*, **69**, 208–9.
Marshall, D. B. & Evans, A. G. (1985). *J. Amer. Ceram. Soc.*, **68**, 225–31.
Marshall, D. B. & Oliver, W. C. (1987). *J. Amer. Ceram. Soc.*, **70**, 542–8.
Marshall, D. B., Cox, B. N. & Evans, A. G. (1985). *Acta Met.*, **33**, 2013–21.
McCartney, L. N. (1987). *Proc. R. Soc. Lond.*, **A409**, 329–50.
Phillips, D. C. & Davidge, R. W. (1986). *Br. Ceram. Trans. J.*, **85**, 123–30.
Prewo, K. M. (1986). *J. Mat. Sci.*, **21**, 3590–600.
Prewo, K. M. & Brennan, J. J. (1982). *J. Mat. Sci.*, **17**, 1201–6.
Prewo, K. M., Brennan, J. J. & Layden, G. K. (1986). *Bull. Amer. Ceram. Soc.*, **65**, 305–22.
Sbaizero, O. & Evans, A. G. (1986), *J. Amer. Ceram. Soc.*, **69**, 481–6.
Tattersall, H. G. & Tappin, G. (1966). *J. Mat. Sci.*, **1**, 296–301.
Wolstencroft, D. H., Curtis, A. R. & Harescroft, R. I. (1981). *Composites*, **12**, 275–83.
Yuh, E. L. & Evans, A. G. (1987). *J. Amer. Ceram. Soc.*, **70**, 466–9.